Preprints of the 19th World Congress
The International Federation of Automatic Control
Cape Town, South Africa. August 24-29, 2014

A Double-loop Control Structure for Tracking Control and Disturbance Attenuation

Mi-Ching Tsai*, Fu-Yun Yang and Chun-Lin Chen

** Department of Mechanical Engineering, National Cheng Kung University, Tainan 701, Taiwan (Tel: +886-6-2352344; e-mail: mctsai@mail.ncku.edu.tw).*

Abstract: The development of high performance controllers capable of dealing with both tracking control and disturbance rejection has attracted considerable attention. This paper investigates the two-degree-of-freedom control structures with a disturbance observer and command feedforward control, respectively, and presents a double-loop control structure. The proposed control structure allows intuitive and independent tuning of disturbance rejection as well as tracking performance. Experimental results obtained from an illustrated servo control system are given to demonstrate the effectiveness and feasibility of the double-loop control structure and design methodology.

Keywords: Disturbance observer, Two-degree-of-freedom control, H-infinity control, Dynamic Stiffness

1. INTRODUCTION

The increasing demand for high performance servo control systems has attracted considerable attention since the dynamic equations of a mechanical system often have external disturbances and/or system uncertainties in practice. Figure 1 illustrates a general double-loop control structure in which the internal-loop compensator aims for robustness, and the external-loop controller is for achieving desired tracking performance (Kim *et al*., 2002) (Kim *et al*., 2003).

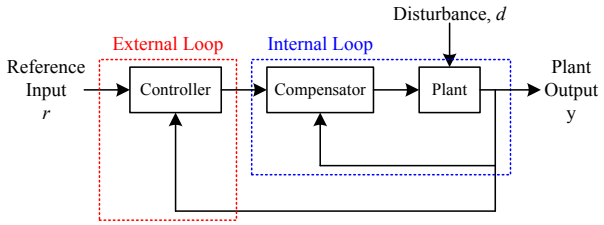

Fig. 1 2DOF control structure.

It is known that the disturbance observer (DOB) design (Ohishi *et al*., 1987) (Tsai *et al*., 2009) is an effective method in which the external disturbance can be estimated and then compensated in the feedback control. An archetypal configuration of the DOB in terms of a two-degree-of-freedom (2DOF) control scheme was proposed by Umeno (Umeno *et al*., 1991). A general DOB structure requires the inverse model of the controlled plant (Tesfaye *et al*., 2000) (Schrijver *et al*., 2002) (Choi *et al*., 2006) (Jones *et al*., 2007). This approach, however, suffers from insufficient robustness since the inverse of the nominal plant model is employed in its framework. To avoid this problem, an alternative framework, namely the model-based disturbance attenuator (MBDA), was proposed for enhancing dynamic stiffness in respect to system parameter variations (Choi *et al*., 1999). A reference feedforward type 2DOF control (RFF-2DOF) was proposed by Yoshio (Yoshio *et al*., 2007), where the feedback controller and feedforward controller could be designed independently. The modified RFF-2DOF, namely model-based reference feedforward (MRFF), was proposed which reveals a comparison of reference and corresponding plant signals for tracking performance (Roppenecker, 2009) (Zeitz, 2012).

It should be noted that the corresponding performance of the external-loop controller in the aforementioned control structures was inevitably affected by the internal-loop compensator due to model uncertainty. The controller design is often a trade-off between reference tracking and disturbance rejection. Generally, MBDA has better disturbance attenuation in low frequency, while MRFF can improve robustness in high frequency. This paper presents a double-loop 2DOF controller structure with dynamic switching to combine both MBDA and MRFF. According to the proposed switching mechanism, the overall control system could be operated as MRFF in the transient and as MBDA in the steady-state, respectively, whereby the benefits of MBDA and MRFF can both be utilized.

2. TWO-DEGREE-OF-FREEDOM CONTROLLER

Let r, d and y be the reference input, external disturbance, and controlled plant output, respectively. Then, the input-output relationships of Fig. 1 are denoted as

$$y = Tr + Dd \,, \tag{1}$$

where T denotes the transfer function from r to y and D is the transfer function from d to y. The tracking performance can be characterized by minimizing the tracking error e

$$e = (1-T)r. \tag{2}$$

The dynamic stiffness function is defined by the inverse of D as a frequency response function, denoted by k_s as

$$k_s(\omega) := \left| D^{-1}(j\omega) \right|, \forall \omega. \tag{3}$$

Thus, maximizing the dynamic stiffness of a servo control system implies minimizing the perturbation caused by external disturbance, while a better dynamic stiffness refers to a larger magnitude of k_s within the performed frequency range. Therefore, the objectives of feedback control design are mainly to make the output y capable of tracking the reference input r and to effectively reject the external disturbance d simultaneously.

2.1 Two-Degree-of-Freedom Controller with MBDA

Figure 2 illustrates the standard unity feedback control system, where P denotes the transfer function of the controlled plant and C is the feedback controller. The transfer functions T and D defined above can be derived as

$$T_I = \frac{PC}{1+PC} \text{ and } D_I = \frac{P}{1+PC}. \tag{4}$$

The controller C can be designed to suppress the external disturbance and eliminate the tracking error simultaneously. This trade-off limits the corresponding performance even if the controller is designed by optimal techniques. An alternative control structure, namely MBDA, was proposed as depicted in Fig. 3, which does not involve the inverse function of the controlled plant to confirm robustness with respect to parameter variations and has better dynamic stiffness to external disturbances. The input-output relationships between r, d, and y of Fig. 3 are given by

$$\begin{aligned} T_M &= \frac{P(1+KP_n)C}{1+PC+PK+PKCP_n}, \\ D_M &= \frac{P}{1+PC+PK+PKCP_n}. \end{aligned} \tag{5}$$

For the case of $P = P_n$, i.e., no modelling error, one has

$$T_M = \frac{P_nC}{1+P_nC}, D_M = \frac{P_n}{(1+P_nC)(1+P_nK)} = D_I\frac{1}{1+P_nK}. \tag{6}$$

It can be concluded from (6) that the external disturbance attenuated by D_I in (4) can be further attenuated by $\frac{1}{1+P_nK}$.

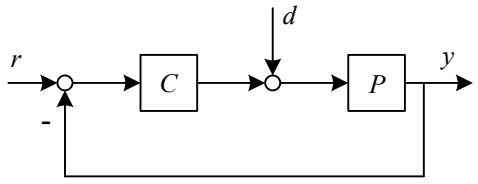

Fig. 2 Standard unity feedback control system.

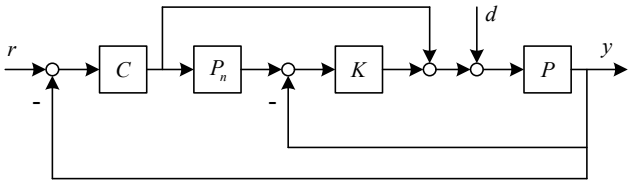

Fig. 3 MBDA control structure.

2.2 Model-Based Reference Feedforward (MRFF) Controller

In practice, the internal-loop compensator K and the external-loop controller C would inevitably affect each other, and the tracking performance would also be abated due to the eigenvalue migration caused from the parameter variations. To reduce the influence and retain the desired performance, consider the control block diagram of the MRFF control structure illustrated in Fig. 4, where

$$T_{MR} = \frac{P(1+KP_n)C}{(1+P_nC)(1+PK)}, \; D_{MR} = \frac{P}{1+PK}. \tag{7}$$

Without modelling error ($P = P_n$), (7) can be simplified to

$$T_{MR} = \frac{P_nC}{1+P_nC}, D_{MR} = \frac{P_n}{1+P_nK}. \tag{8}$$

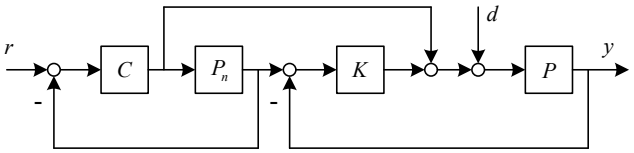

Fig. 4 MRFF control structure.

As can be found from (8), C and K can be designed independently in the MRFF framework so that the controller design would be more intuitive. To characterize the disturbance attenuation of the MRFF, let D_{MR} in (8) be rewritten as

$$D_{MR} = \frac{P_n}{1+P_nK} = \frac{P_n}{1+P_nC}\left(\frac{1+P_nC}{1+P_nK}\right) = D_I\left(\frac{1+P_nC}{1+P_nK}\right). \tag{9}$$

Thus far, one can compare the disturbance attenuation of the control frameworks addressed above. It can be found by the definition of (3) that the dynamic stiffness of the MBDA from (6) can be calculated by

$$k_M = \left|D_M^{-1}\right| = \left|\frac{1+P_nK}{P_n}(1+P_nC)\right|. \tag{10}$$

The dynamic stiffness of MRFF can be derived from (9) as

$$k_{MR} = \left|D_{MR}^{-1}\right| = \left|\frac{1+P_nK}{P_n}\right|. \tag{11}$$

Then, the dynamic stiffness of the MBDA is greater than that of MRFF if P_nC is designed such that

$$\left|1+P_nC\right| > 1, \forall\omega. \tag{12}$$

On the contrary, the robust stability of MRFF would be better than MBDA, which is illustrated in the following.

3. DOUBLE-LOOP CONTROL STRUCTURE

3.1 Double-Loop 2DOF Controllers

Notice that the MBDA depicted in Fig. 3 can achieve better dynamic stiffness with respect to system variations, while the

benefit of the MRFF controller depicted in Fig. 4 lies in controller design for tracking performance and better robustness. However, the MRFF controller can be easily switched to the MBDA, or vice versa from the MBDA to the MRFF. This leads to the development of a new double-loop control structure as depicted in Fig. 5, where Ψ is introduced for switching these two 2DOF controllers dynamically.

Now consider the double-loop structure of Fig. 5. One has

$$T_P = \frac{PC(1+KP_n)}{1+PK+P_nC+P_nCPK+C(P-P_n)\Psi},$$
$$D_P = \frac{P[1-C(\Psi-1)P_n]}{1+PK+P_nC+P_nCPK+C(P-P_n)\Psi}, \quad (13)$$

where Ψ is chosen as a low-pass filter, i.e., $\Psi = \frac{1}{\tau s+1}$.

Thus, for the case of $\lim_{s\to\infty}\Psi(s)=0$

$$T_P = T_{MR} = \frac{P(1+KP_n)C}{(1+P_nC)(1+PK)}, D_P = D_{MR} = \frac{P}{1+PK}, \quad (14)$$

and for the case of $\lim_{s\to 0}\Psi(s)=1$

$$T_P = T_M = \frac{P(1+KP_n)C}{1+PC+PK+PKCP_n},$$
$$D_P = D_M = \frac{P}{1+PC+PK+PKCP_n}. \quad (15)$$

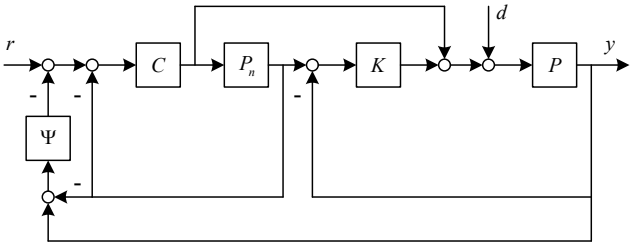

Fig. 5 Double-loop control structure.

In the transient state, i.e., for the frequency such that $\tau\omega >> 1$ and $|\Psi(j\omega)| \approx 0$, the control structure of Fig. 5 would be dominated by the MRFF in which the controller should be designed for the desired tracking performance. In the steady state, i.e., for the frequency such that $\tau\omega \approx 0$ and $|\Psi(j\omega)| \approx 1$, the proposed structure of Fig. 5 would be identical to the MBDA in which the controller should be designed for the specified dynamic stiffness.

The design objectives of K, C and Ψ in the double-loop control system are summarized as follows:

i. C should be designed such that $\left|\frac{P_nC}{1+P_nC}(j\omega)\right| \approx 1$ for the desired tracking control performance.

ii. The design of K is aimed to reduce $\left|\frac{P}{1+PK}(j\omega)\right|$ within the bandwidth of interest for improving dynamic stiffness, and the external loop response should not be influenced by K.

iii. The bandwidth of the low-pass filter Ψ, characterized by the time constant $\tau > 0$, should be chosen appropriately to specify the desired switching between MBDA and MRFF.

It should be noted that the characteristic equation of the proposed double-loop 2DOF control system is the same as that of MBDA for $P = P_n$. Since Ψ, T_{MR} and D_{MR} are stable functions by the assumption, it can be concluded that the nominal stability of the proposed mixed two-loop 2DOF controller structure is guaranteed with the same control parameters as MRFF.

3.3 Robust Performance

Furthermore, consider a perturbed system expressed by $P = P_n(1+\Delta_P)$, where Δ_P is an allowable multiplicative uncertainty. Assuming that the closed-loop system in (7) is stable, a sufficient condition for the robust stability of Fig. 6 is given by the small gain theorem as

$$\left|\Delta_p\right|_{s=j\omega} < \left|\Omega_P\right|_{s=j\omega}, \forall\omega, \quad (16)$$

where

$$\Omega_P = \frac{(1+P_nK)(1+P_nC)}{P_nK+P_nCP_nK+CP_n\Psi}. \quad (17)$$

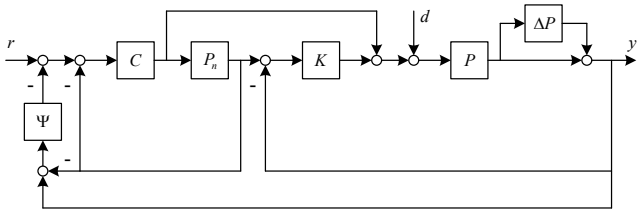

Fig. 6 Variable structure control with model uncertainty.

Similarly, the robustness of MBDA and MRFF can also be derived by (5) and (7), respectively, as

$$\Omega_M = \frac{(1+P_nK)(1+P_nC)}{P_nC+P_nK+P_nCP_nK}, \quad (18)$$

and

$$\Omega_{MR} = \frac{(1+P_nK)}{P_nK} = \frac{(1+P_nK)(1+P_nC)}{P_nK+P_nCP_nK}. \quad (19)$$

It can be concluded from (17), (18), and (19) that, if the controller C is designed such that

$$\left|P_nK+P_nCP_nK\right| < \left|P_nK+P_nCP_nK+P_nC\right|, \forall\omega, \quad (20)$$

then the framework of MRFF has better robust stability than that of MBDA. The proposed double-loop control structure processes the hybrid framework by means of the auxiliary filter, which benefits engineers by allowing the controller parameters to be designed aggressively against specific

disturbances and achieve enhanced tracking behavior with higher robustness.

3.3 An Illustrated Design Example

To demonstrate the effectiveness of the double-loop control system and its design methodology, consider an illustrated design example whose nominal model is given by

$$P_n(s)=\frac{b_n}{s+a_n}. \tag{21}$$

As mentioned earlier, the nominal stability of the proposed structure is guaranteed with the same parameterization of MRFF. As an illustrated design of the MRFF controller in Fig. 7, let C be a pseudo-derivative feedback (PDF) controller and K a classical PI compensator. Note that the constant gains $[K_I \quad K_P]$ of the PI compensator can be solved for satisfying the desired dynamic stiffness, while the constant gains $[C_I \quad C_P]$ of the PDF controller can be easily computed for satisfying the desired tracking performance.

To characterize the controller parameters $[C_I \quad C_P]$, one can see from Fig. 7 that the transfer function from r to y^*, denoted as $M(s)$, for $a=a_n$ and $b=b_n$, can be derived as

$$M(s)=\frac{C_I b_n}{s^2+(a_n+C_P b_n)s+C_I b_n}=\frac{\omega_n^2}{s^2+2\xi\omega_n s+\omega_n^2}. \tag{22}$$

Since $M(s)$ is a standard second-order system, the parameters $[C_I \quad C_P]$ can be found directly from the natural frequency ω_{nc} and the damping ratio ξ_c. For the case of $a_n=2.5$, $b_n=17000$, and the desired $\omega_{nc}\approx 30\ rad/s$ and $\xi_c\approx 0.866$, one has $C_I=0.053$ and $C_P=0.003$.

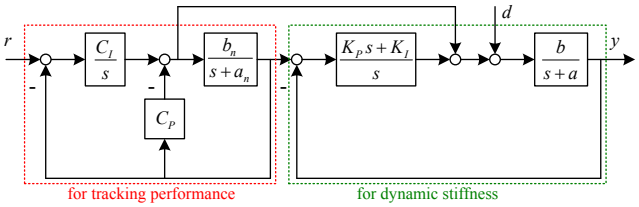

Fig. 7 Design example of MRFF control structure.

As depicted earlier, despite the transfer function from r to y being affected only by controller C for $P=P_n$, the corresponding performance of the external-loop controller was in reality inevitably affected by the internal-loop compensator. Therefore, as a rule of thumb, the bandwidth of the internal-loop feedback system should be designed to be 3 to 5 times greater than that of the external-loop in a cascade design approach, i.e., the bandwidth of $\frac{P_n K}{1+P_n K}$ should be 3 to 5 times greater than that of $\frac{P_n C}{1+P_n C}$. In this case, the bandwidth of the internal loop is chosen by $\omega_n=150\,rad/s$ and $\xi=1$, which leads to $K_P=0.0175$ and $K_I=1.32$.

Figure 8 illustrates the magnitude of the Bode plot for charactering the dynamic stiffness and robustness resulting from MBDA and MRFF, as well as the double-loop control structure with different τ depicted in Fig. 9. As expected from (10) and (11), the framework of MBDA possesses a higher dynamic stiffness than MRFF, while the frequency is below $100\,rad/s$. Furthermore, as can be found from (17), (18), and (19), the robustness of MRFF is better than MBDA when (20) is satisfied, while the proposed structure has a trade-off between those frameworks. Therefore, to maintain better disturbance attenuation with performed tracking performance, the parameter of τ is chosen as 0.01.

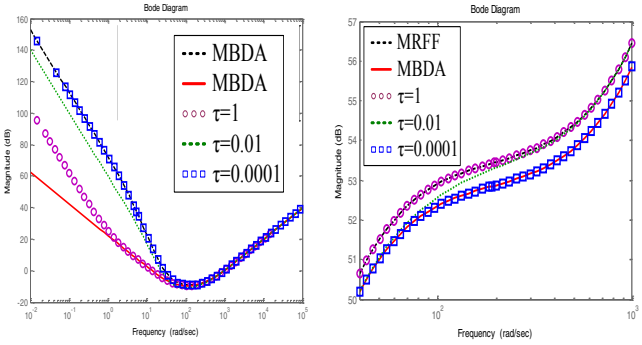

(a) Dynamic Stiffness (b) Robustness

Fig. 8 Dynamic stiffness and robustness with respect to different τ.

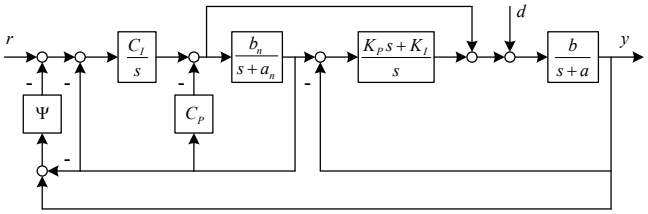

Fig. 9 Design example of double-loop control structure.

In this illustrated example, a design procedure of the double-loop control structure is summarized as follows, of which the desired bandwidth is beyond 25 rad/s.

i. Set the damping ratio ξ_c and the designed bandwidth ω_{nc}, then one has $[C_I \quad C_P]$.

ii. Choose K_P and K_I such that the internal loop is provided with a satisfactory bandwidth, which is about 5 times the external loop.

iii. Plot the dynamic stiffness of MRFF and MBDA; then, choose τ for setting the bandwidth of Ψ.

4. EXPERIMENTAL RESULTS

To show the effectiveness of the proposed structure and its design methodology, a rotary servomotor is adopted for the

experimental study. As shown in Fig. 10, the servomotor is connected with the hysteresis brake system via a flexible coupling. Therefore, the external disturbance can be realized by controlling the hysteresis brake. A simplified model of the servomotor without the mechanical coupling is obtained with parameters the same as in the illustrated example.

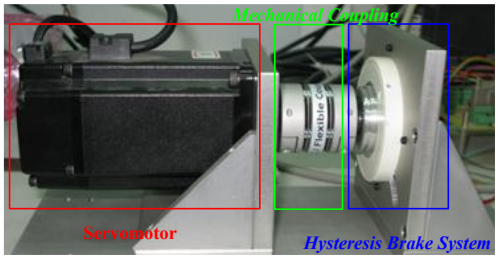

Fig. 10 Servomotor with hysteresis brake.

Therefore, for the designed bandwidth of velocity loop $\omega_{nc} \approx 30 rad/s$ and $\xi_c \approx 0.866$, the controller parameters are given by $C_I = 0.053$, $C_P = 0.003$, $K_P = 0.0175$, $K_I = 1.32$, and $\tau = 0.01$. Figure 11 shows the corresponding response of each framework without the mechanical coupling and brake system, in which the input commands are 30rpm and 2000rpm, respectively. It can be found from (4), (6), (8), and observed from Fig. 11 that the three frameworks have almost the same transient behavior, while the nominal model P_n is close to P.

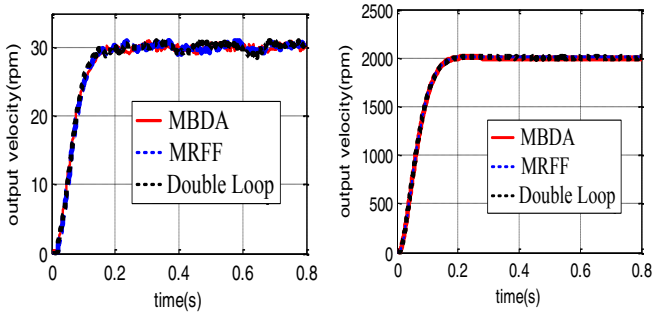

(a) r=30 rpm (b) r=2000 rpm

Fig. 11 Step response without mechanical coupling.

Figure 12 shows the corresponding response of each framework with mechanical coupling, in which the mechanical coupling is not identified as a part of the plant, but rather for characterizing the model uncertainty. It can be concluded that, via comparing Fig. 11 and Fig. 12, the MRFF processes the best transient response with respect to the model uncertainty, and the output velocity of MBDA tends to oscillate while the controlled plant is dominated by the external friction and nonlinearity at low speeds.

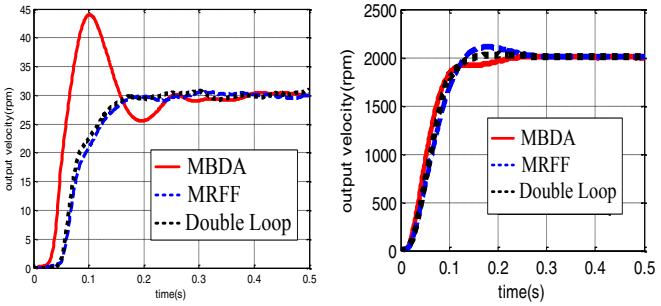

(a) r=30 rpm (b) r=2000 rpm

Fig. 12 Step response with mechanical coupling.

For the verification of the disturbance rejection, a sinusoid disturbance of $0.1+0.1\sin(2\pi ft)\,N$ with $f = 0.5$ enters the system in the steady-state via the hysteresis brake system, with the experimental results demonstrated in Fig. 13. As depicted from (10) and (11), external disturbance in low frequency achieved satisfactory attenuation in MBDA, while the disturbance rejection performance of the proposed double-loop control structure can be easily enhanced via reducing the value of τ, as depicted in Fig. 8.

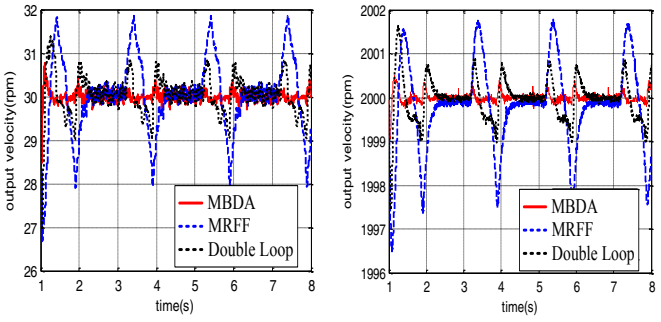

(a) r=30 rpm (b) r=2000 rpm

Fig. 13 Disturbance rejection of each framework.

Furthermore, for the verification of disturbance rejection in transient behavior Fig. 14 illustrates the step response with mechanical coupling while the abovementioned sinusoid disturbance enters the system at the outset. Note that the external disturbance is generated by the hysteresis brake system. This means that there is only resistance force, namely, a varied friction. As can be expected from the dynamic plot of Fig. 8, the dynamic stiffness of MRFF is much lower than MBDA in low frequency, while the external disturbance leads to an extra friction and increases the rising time of MRFF, as illustrated in Fig. 14. The MBDA has better dynamic stiffness with respect to the external disturbance but less robust performance. The proposed double-loop control structure, which integrates the advantages of both frameworks, can stipulate the designed specifications with satisfying dynamic stiffness and process the most satisfied transient response while the model variation and external disturbance occur simultaneously, and can be intuitively designed via the framework of MRFF and the time constant τ.

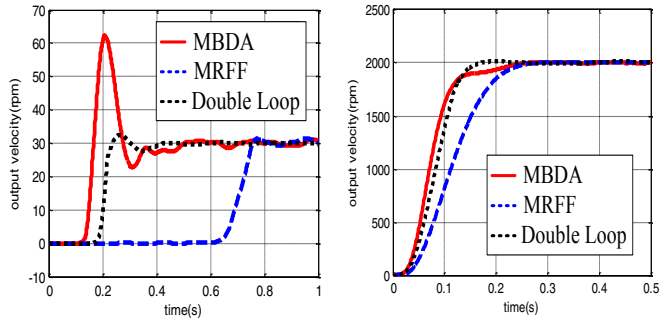

(a) r=30 rpm (b) r=2000 rpm

Fig. 14 Step response with external disturbance.

5. CONCLUSION

This paper presented an application-oriented study in which 2DOF controllers were compared and analyzed. For the purpose of intuitive and independent tuning, the framework of a MRFF controller, which exhibits better robustness, was first investigated, while the MBDA has greater dynamic stiffness. By virtue of this, an advanced control structure was proposed as a double-loop of the MRFF controller and MBDA, which provides more design flexibility and benefits engineers by allowing the controller parameters to be designed aggressively against specific disturbances and achieve suitable performed tracking behavior. The 2DOF controller design of the proposed double-loop framework is simple and intuitive. The validity of the proposed framework and design method was verified by experimental results. Although the design process is developed for a specific case, the proposed double-loop control structure is applicable to more complicated systems with various implementations.

ACKNOWLEDGMENT

This work was supported by National Science Council (NSC) of Taiwan, under project NSC 100-2923-E-006-005-MY3.

REFERENCES

Choi, B.K., Choi, C.H. and Lim, H. (1999). Model-based disturbance attenuation for CNC machining centers in cutting process. *IEEE/ASME Transactions on Mechatronics*, vol. 4, pp. 157-168.

Choi, H.T., Kim, B.K. and Eom, K.S. (2006). A new framework for two loop disturbance rejection control. *International Journal of Control*, vol. 79, pp.636-649.

Hu, J.S., Yin, D. and Hori, Y. (2011). Fault-tolerant traction control of electric vehicles. *Control Engineering Practice*, vol. 19, pp. 204-213.

Jones, R.W. and Tham, M.T. (2007). Disturbance observer design for continuous system with delay. *Asia-Pacific Journal of Chemical Engineering*, vol. 2, pp. 517-525

Kim, B.K., Choi, H.T., Chung, W.K. and Suh, I.H. (2002). Analysis and design of robust motion controllers in the unified framework. *Journal of Dynamic Systems, Measurement, and Control*, vol. 124, pp. 313-321.

Kim, B.K. and Chung, W.K. (2003). Advanced disturbance observer design for mechanical positioning systems. *IEEE Transactions on Industrial Electronics*, vol. 50, pp. 1207-1216.

Ohishi, K., Nakao, M., Ohnishi, K. and Miyachi, K. (1987). Microprocessor-controlled DC motor for load-insensitive position servo system. *IEEE Transactions on Industrial Electronics*, vol. IE-34, pp. 44-49.

Roppenecker, G. (2009). Zustandsregelung lineare Systeme-eine neu-betrachtung. *Automatisierungstechnik 57*, pp. 491-498.

Schrijver, E. and Dijk, J.V. (2002). Disturbance observer for rigid mechanical systems: equivalence, stability, and design. *Journal of Dynamic Systems, Measurement, and Control*, vol. 124, pp. 539-548.

Tesfaye, A., Lee, H.S. and Tomizuka, M. (2000). A sensitivity optimization approach to design of a disturbance observer in digital motion control systems. *IEEE/ASME Transactions on Mechatronics*, vol. 5, pp.32-38.

Tsai, M.C., Hu, J.S. and Hu, F.R. (2009). Actuator fault and abnormal operation diagnoses for auto-balancing two-wheeled cart control. *Mechatronics,* vol. 19, pp. 647-655.

Umeno, T. and Hori, Y. (1991). Robust speed control of DC servomotors using modern two degrees-of-freedom controller design. *IEEE Transactions on Industrial Electronics*, vol. 38, pp. 363-368.

Yoshio, E., Yoshinori, F., Fujiwara, T. and Masayuki, S. (2010) 2DOF control system design for manoeuvrability matching and gust disturbance rejection in in-flight simulator MuPAL-α. *SICE Annual Conference*, pp. 524-528.

Zeitz, M. (2012) Vorsteuerungs-entwurf im Frequenzbereich: offline oder online. *Automatisierungstechnik 60*, pp. 375-383.